IDENTIFICATION OF MATERIALS USING AERIAL HYPERSPECTRAL IMAGES

BEKŐ, LÁSZLÓ
HUNYADI, GERGELY
LAAKSO, KATI
NYGRÉN, PETRI

Summary

The aerial hyperspectral imagery has a large information content and contains data not just only in the visible light spectra but in the near-infrared and the short-wave infrared spectra as well. Due to this, the technology is applicable to examine and detect preferences and conditions that visible identification is not possible or limited. During the last decade, hyperspectral imagery was successfully used for the analysis of vegetation, soil or minerals. During our research the AISA Fenix1K hyperspectral sensor of the Research Institute was used for data collection with the collaboration of experts from the Finnish sensor producer company near to Siófok. The collected aerial hyperspectral data and the ground spectral data as reference were compared and a spectral library of the examined materials was developed for future classifications. The ability to separate various materials was examined with statistical analyses with which we can determine the spectral separability of target objects. The analysis was fulfilled on the original and on transformed channels as well. According to the results we can conclude that the transformed channels are more applicable to separate these materials which was demonstrated on scatter plots too.

Keywords: hyperspectral, airborne remote sensing, target detection, ground truth acquisition, separability
JEL: C89

Introduction

Hyperspectral imagery (HSI) may contain hundreds of continuous narrow spectral bands that gives the possibility to detect and separate various materials more precisely comparing with the traditional broadband multispectral imagery. HSI is suitable for various military and civil applications. During the last two decades the main aim of remote sensing was the detection of target spectrums (natural and artificial objects) that spectral characteristics were affected by the background. The advantages of HSI give the possibility to separate these and similar characteristics more precisely by using large spectral resolution. (Wei et. al., 2015). One of the main applications of aerial hyperspectral assessment is object exploration that can be a problem of reckoning among two groups (searched material or not). The spectral characteristics of each pixel indicate the presence of target spectra or the spectral characteristics of the background are deterministic. Many classification methods are available to solve this, for example the Support Vector Machine (Boser et. al. 1992) which algorithm gives good results during the classification of hyperspectral images (Gualtieri – Cromp, 1999; Melgani – Bruzzone, 2004). Researchers have used other directed classification algoritms to detect target spectrums as well (Yanfeng et. al., 2015; Leblanc et. al., 2014). The examination of spectral separability of target spectrums (materials) is essential to select the suitable

classification algorithm (Tobak et. al., 2012). The aim of this paper is a statistical analysis to prepare and support the determination of various target materials and target spectrums. During our research we examined the spectral familiarities and differences of various materials by using aerial hyperspectral imagery and on-field measurements.

Material and methods

Study site

The study area is located in the southern shoreline of Balaton, nearby Siófok, Papkutapszta airport (LHPK) (*figure 1*) (46°52.266' N, 18°2.419' E). The investigated materials (22 pc.) were arranged on northern end of the runway, separated from each other.

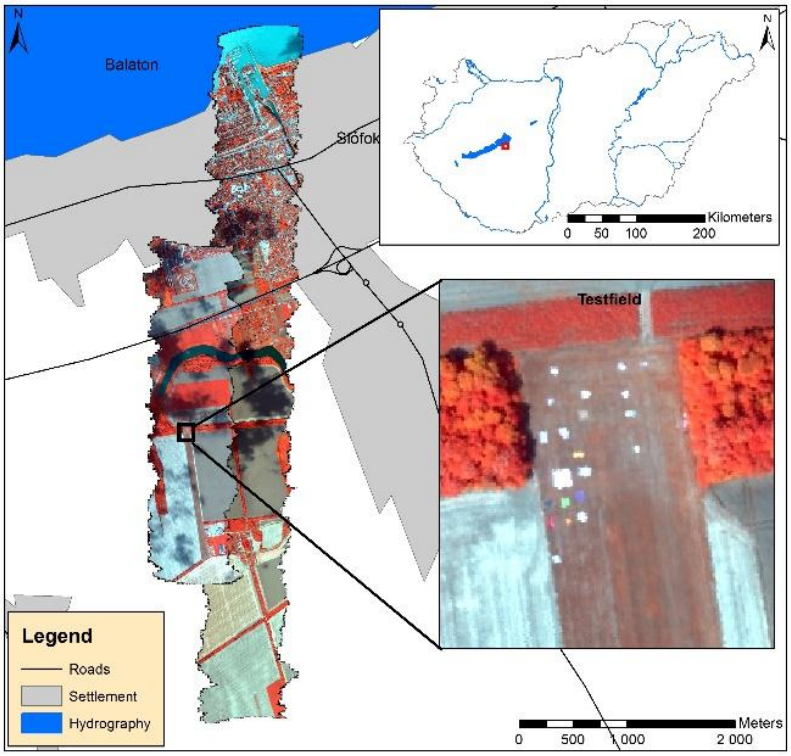

Figure 1: Location of the study site
Source: Own editing, 2016

Airborne hyperspectral data

The images were taken by the AISA Fenix1k (www.specim.fi) hyperspectral sensor during the flight campaign. The data acquisition was done on 10.07.2015 between noon and 1 pm with light cumulus coverage. The given aerial data was applicable for further analyses because the study site was not affected by shadows of clouds. The sensor was implemented to a Cessna C206 airplane. During the campaign the altitude was 3350ft

(AGL) which resulted 70 cm ground resolution. The data was collected in 380-2450 spectral range with 7 nm spectral sampling on 333 spectral bands. The sensor system is built together with a high precisions GNSS/INS system (Oxford OxTS3010) which is gives position and navigation data for georeferencing. The pre-process of data was done by CaligeoPRO v2.2.4 which works in the frame of IDL. The data was processed with ENVI 5.0 software.

Ground-based hyperspectral data

In the same time of the aerial data acquisition on-field data was collected with ASD FieldSpec3 spectrophotometer in the same spectral range as reference data. The accurate coordinates of the objects were collected with a DGPS to ensure the comparability of aerial and on-field data. A spectral library was built by processing the collected data of target objects. The set of examined materials on the study site is shown on *figure 2*.

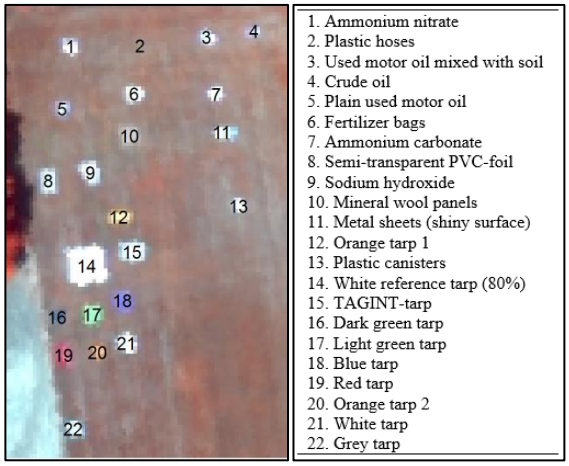

Figure 2: Test field targets

Data processing

The hyperspectral data was pre-processed with CaligeoPRO and processed with ENVI 5.0. The noisy channels and (because of the effect of cumulus) the short wave infrared spectral range were removed from the aerial images which resulted that 92 spectral bands were involved during data process. The reflectance curves of on-field data and aerial images were compared and the typical spectral ranges were determined.
The separability of materials was examined with Jeffries-Matusita (J-M) Distance which means the comparison of materials in pairs. (Matusita, 1966; Ersboll, 1988). During the method the distribution functions were compared. The values differed between 0 and 2, where 2 means large separability.

The values were calculated with the following equation:

$$\alpha = \frac{1}{8}(\mu_i - \mu_j)^T \left(\frac{C_i + C_j}{2}\right)^{-1} (\mu_i - \mu_j) + \frac{1}{2} ln \left(\frac{|(C_i + C_j)/2|}{\sqrt{|C_i| \times |C_j|}} \right)$$

$$JM_{ij} = \sqrt{2(1 - e^{-\alpha})}$$

Where: i and j = two signature (materials) being compared
C_i = covariance matrix of signature i
m_i = mean vector of signature i
ln = natural logarithm function
$|C_i|$ = determinant of C_i (matrix algebra)
Source: Swain-Davis, 1978

On the hyperspectral image signal amplifying and information increase were done by Minimum Noise Fraction (MNF) transformation. MNF transformation reduces the dimension-number of hyperspectral data while filters noisy fractions. This linear transformation contains two Principal Component Analysis (PCA) that follow each other. The first one removes the noisy and recalculate the data. This results unit variance of noise and linearly independent bands. The second one is a simple principal component analysis which is done on the image where the noise is removed. By further grouping the given MNF bands we can produce the required number of target spectrums (endmembers) (Green et al, 1988). The J-M distance values were calculated in the case of the original hyperspectral image and also on the transformed bands.

Results

Comparing the spectrums given by the aerial images and on-field measurements the two curves may show large differences. This is mainly resulted by the circumstances of on-field measurements which is similar to the homogenous laboratory conditions - the detector is close to the examined material. In contrast with this, during aerial imagery between the detector and the examined material there was a 1100 m thick air (water vapour, dust particles, etc.) which influences the detected spectrums. These affects can be reduced with atmospheric correction. In these conditions, the minimum and maximum reflectance and absorption range of each material can be determined in both cases (aerial imagery and on-field measurements) (*figure 3*).

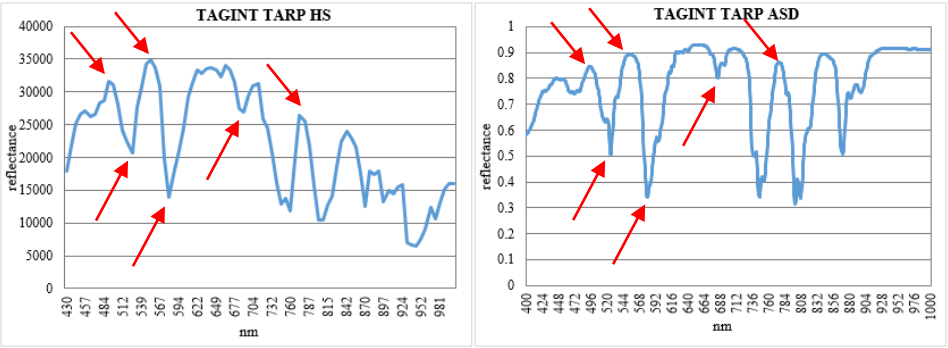

Figure 3: Spectrums of Tagint tarp surveyed by aerial hyperspectral technology and ground based measurement

On the aerial images taken in visible the separation of examined materials (sodium hydroxide, ammonium carbonate, white tarp etc.) is limited or impossible. In the case of those materials which seemed similar on the RGB images we calculated the J-M distance and represented the results in matrix (*table 1*).

Table 1: J-M separability measures between management materials (original bands)

Materials	1	2	3	4	5	6	7	8	9	10
1	0									
2	2.00	0								
3	1.99	2.00	0							
4	2.00	1.97	2.00	0						
5	2.00	1.94	2.00	**1.80**	0					
6	1.97	1.96	1.99	1.99	1.99	0				
7	2.00	2.00	2.00	2.00	2.00	2.00	0			
8	2.00	1.99	2.00	2.00	1.99	1.99	2.00	0		
9	2.00	**1.72**	1.99	1.96	1.90	1.96	2.00	1.99	0	
10	2.00	1.94	1.99	1.98	1.91	1.98	2.00	2.00	1.95	0

1: Ammonium nitrate; 2: Fertilizer bags; 3: Ammonium carbonate; 4: Semi-transparent PVC-foil; 5: Sodium hydroxide; 6: Plastic canisters; 7: 80% white reference tarp; 8: TAGINT tarp; 9: White tarp; 10. Metal sheets with shiny surface

Based on the original hyperspectral data the minimum separability was in the case of fertilizer bags and white tarp and the semi-transparent PVC-foil and sodium hydroxide which indicates the error during the classification of these materials.

The separability of materials was examined in the case of MNF transformed channels as well. The result matrix is shown on *table 2*. The J-M distance calculation with the MNF bands showed larger separability of the examined materials which increases the accuracy of classification.

Table 2: J-M separability measures between management materials (MNF bands)

Materials	1	2	3	4	5	6	7	8	9	10
1	0									
2	2.00	0								
3	2.00	2.00	0							
4	2.00	1.99	2.00	0						
5	2.00	**1.98**	2.00	**1.98**	0					
6	2.00	2.00	2.00	2.00	2.00	0				
7	2.00	2.00	2.00	2.00	2.00	2.00	0			
8	2.00	2.00	2.00	2.00	2.00	2.00	2.00	0		
9	2.00	2.00	2.00	2.00	2.00	2.00	2.00	2.00	0	
10	2.00	2.00	2.00	2.00	2.00	2.00	2.00	2.00	2.00	0

1: Ammonium nitrate; 2: Fertilizer bags; 3: Ammonium carbonate; 4: Semi-transparent PVC-foil; 5: Sodium hydroxide; 6: Plastic canisters; 7: 80% white reference tarp; 8: TAGINT tarp; 9: White tarp; 10. Metal sheets with shiny surface

The matrix shown in table 2 can be abstracted graphically as a projection to the selected layout of the MNF transformed data. If the selected spatial classes are examined in this transformed spectral space, on a 2-dimensional scatter-plot, we can find and separate the classes with larger accuracy (larger spectral separability). In this intensity space, pixels with similar spectral characteristics can be found in one group. These groups can be segregated from each other (*figure 4*).

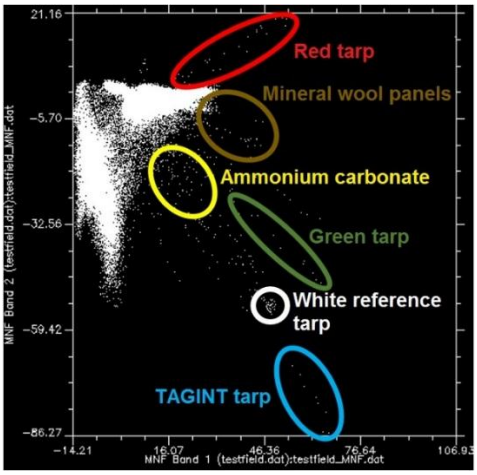

Figure 4: Scatter plot of MNF1 and MNF2 bands

Conclusion

The aim of this research was the examination of applicability of aerial hyperspectral images to separate and classify various materials. To analyse this, the spectral library of these materials (based on on-field spectral measurements in the same time as the flight campaign) was prepared which can be used to detect these materials independently of their location. During the statistical analysis related to the spectral classification of these materials we concluded that the use of visual interpretation of original images and the

calculation of J-M distance do not give acceptable results in the case of two material pairs (fertilizer bag - white tarp, semi-transparent PVC-foil - sodium hydroxide). This means similar spectral characteristics of these materials which may indicate errors during classification.

By increasing the information content of images with MNF transformation and using the given data, the separation accuracy of materials also increased. The examined materials can be classified spectrally which explains the use of transformed channels during target spectrum classification. The next step of our research is testing the applicability of various classification algorithms by using the determined target spectrums.
The collected aerial hyperspectral images and on-field data is suitable for research on the field of agriculture, environmental management and atmospheric corrections.

Acknowledgements

This study was supported by TÁMOP-4.2.2.D-15/1/KONV-2015-0010 'Távérzékelési és zöldenergia témájú célzott komplex alapkutatási programok előkészítése, hálózatosodás és felkészülés nemzetközi programokban és kezdeményezésekben való részvételre' grant scheme.

References

[1.] Boser, B.E. – Guyon, I.M. – Vapnik, V.N. (1992): A training algorithm for optimal marginclassifiers. In: *Proceeding Fifth Annual Workshop Computer Learn*. Theory, ACM, 144–152 pp.

[2.] Ersboll, B.K. (1988): Transformations and Classifications of Remotely Sensed Data: Theory and Geological Cases, PhD Thesis, Department of Mathematical Modelling, Technical University of Denmark, 297pp

[3.] Green, A.A. – Berman, M. – Switzer, P. – Craig, M.D. (1988): A Transform for Ordering Multispectral Data in terms of Image Quality with Implications for Noise Removal, *IEEE Transaction Geoscience and Remote Sensing*, vol. 26, No. 1, 65-74 pp.

[4.] Gualitier, J.A. – Cromp, R.F. (1999): Support vector machines for hyperspectral remote sensing classification. In: Proceeding SPIE, *International Society for Optics and Photonics*, 221–232 pp.

[5.] Leblanc, G. – Kalacska, M. – Soffer, R. (2014): Detection of single graves by airborne hyperspectral imaging, *Forensic Science Int.*, vol. 245, 17-23 pp.

[6.] Matusita, K. (1966): A distance and related statistics in multivariate analysis. In: (ed.) Krishnaiah, P.R.: *Multivariate Analysis*. Academic Press, New York, 187-200 pp.

[7.] Melgani, F. – Bruzzone, L. (2004): Classification of hyperspectral remote sensing images with support vector machines, *IEEE Transaction Geoscience and Remote Sensing*, vol. 42, 778–1790 pp.

[8.] Swain, P.H. – Davis, S.M. (1978): *Remote Sensing: The Quantitative Approach.* New York, McGraw Hill Book Company.

[9.] Tobak Z. – Csendes B. – Henits L. – van Leeuwen B. – Szatmári J. – Mucsi L. (2012): Városi felszínek spektrális tulajdonságainak vizsgálata légifelvételek lapján, In: "VI. Magyar Földrajzi Konferencia", SZTE – TFGT, Szeged, 1088-1097 pp.

[10.] Wei, L. – Quin, D. – Bing, Z. (2015): Combined sparse and collaborative representation for hyperspectral target detection. *Pattern Recognition*, vol. 48, 3904-3916 pp.
[11.] Yanfeng, G. – Yuting, W. – He, Z. – Yue, H. (2015): Hyperspectral target detection via exploiting spatial-spectral joint sparsity, *Neurocomputing*, vol. 169, 5-12 pp.

Authors:

Bekő, László
Researcher/PhD student
Research Institute of Remote Sensing and Rural Development/ Institute of Earth Sciences
Károly Róbert College/ University of Debrecen
ifj.beko.laszlo@gmail.com

Hunyadi, Gergely PhD
Research engineer
Envirosense Hungary Ltd.
ghunyadi@gmail.com

Laakso, Kati PhD
Research engineer
Specim, Spectral Imaging Ltd.
kati.laakso@specim.fi

Nygrén, Petri
Sales Manager
Specim, Spectral Imaging Ltd.
petri.nygren@specim.fi